TASK QUARTERLY 7 No 4 (2003), 479–498

ARCHING BEHAVIOUR OF COHESIVE POWDERS IN A PILOT-SCALE PLANE-FLOW SILO

ROBERT J. BERRY[1], ANTHONY H. BIRKS[1,2] AND MICHAEL S. A. BRADLEY[1]

[1] *Wolfson Centre for Bulk Solid Handling Technology, University of Greenwich, Woolwich, London, SE18 6BU, UK*
br04@gre.ac.uk, ba02@gre.ac.uk, bm08@gre.ac.uk

[2] *PTE, 2 Goldsel Road, Swanley, Kent, BR8 8EZ, UK*
ahbirks@ahbirks.free-online.co.uk

(Received 10 July 2003)

Abstract: The paper records some of the results and observations from a pilot scale plane-flow silo with a variable geometry hopper and a fully width slot outlet. The original objectives were simply to study the shape of arches and their failure mechanisms under a range of conditions. However, the behaviour of arches did not conform to the conventional assumptions and neither did other silo behaviour. The paper contains a summary of the main findings of this work, but concentrates on the arches formed under mass-flow and non-mass-flow geometries for the filling condition.

Keywords: plane-flow silo, variable geometry hopper, filling condition, arch shape, critical arch dimension

1. Introduction

The initial objectives of the doctoral project were to measure the shapes of arches under a range of hopper geometries using a scanning laser-ranging device positioned directly under the arch and to determine the mechanisms of arch failure by high-speed photography. As all previous literature referring to silo arches [1–7] had implicitly assumed the notional form of the arch (shown later in Figure 4), the authors were totally unprepared for the type of arch and flow behaviour discovered. This lack of information also meant that the x-y scanning table was not fully appropriate for its duty and an x-θ scanning arrangement would have been better. Apart from the reasonably smooth arch formed by tensile fracture of the bulk solid, after retraction of the hopper gate, the subsequent results totally destroyed both the notion of the conventional arch and the considered wisdom that emptying a small quantity of powder from the hopper section created a truly emptying state. The additional volume

of data and observations of unexpected behaviour caused the high-speed photography to be dropped.

This paper describes the main points of construction of the pilot-plant plane-flow silo with a fully variable geometry hopper and presents a portion of the large volume of results and observations on the effect of a range of outlet sizes and hopper slopes on the arches formed by three cohesive bulk solids. These bulk solids were, olivine sand (mixed with an aqueous solution of glycerol and allowed to dry, to provide tensile stress), a fly ash and a hydrated lime.

From the initial arching experiments, it was found to be necessary to make clear distinctions between three different states that occur within the stored bulk solids. These were:

- "at filling",
- "at transition",
- "at emptying".

While there is no sharp boundary between the conditions, the distinctions are essential to the objective discussion of the observed behaviour and are labelled in this way to distinguish them from the causal use of common terms. The "at filling" condition signifies the elastic and undisturbed content of the hopper that is still the case, when in all instances of test observations, slip has occurred at the wall. At first sight this may appear contradictory, but an extreme example of this behaviour is the slip at the walls that would occur with a bolder of dried clay when the hopper walls were moved apart. In later figures, it will be observed that, after moving the hopper walls apart, the previous arch abutments protrude from the silo outlet.

The "at emptying" condition' is attained only after the main portion of the 'filled' contents of the hopper has been emptied. As the transition zone of the stress-field switch sits mainly below the physical wall transition, it is reasonable to assume that the true "at emptying" condition does not occur until material which has passed through the switch zone and presents at the outlet. If all stress distributions in a mass-flow hopper were of the conventional Jenike type, *i.e.* a diminishing stress on approaching the outlet, it is readily seen that bulk solids in this stress field will be weaker than that in a filling stress field. Just how much stronger bulk solid is in the latter case, we shall see later.

The "at transition" condition is defined for completeness as being any condition not "at filling" nor "at emptying".

The paper briefly describes the design of the silo system in order to appreciate how some of the tests were possible, along with some operational details. A small section reviews the significant findings of the whole project, while finally, the main section details the bulk solid behaviour for the "at filling" condition during outlet widening over a range of hopper angles.

2. Design of the plane flow silo system and its operation

The silo system comprised a wide declined belt discharger on rails so that it could be readily replaced by a computer-controlled scanning laser-ranging unit, a plane-flow hopper of variable geometry, a vertically expandable vertical section,

a mechanically separate bulk solid feeding system. The bulk solid from the belt discharger filled either, a low-loading wagon or, bottom-emptying skips which allowed bulk solid recycling via a hoist. These components had to fulfil the following requirements:

- a stable and symmetric flow throughout silo,
- a controlled, low velocity discharge with uniform extraction across the slot outlet,
- a constant head of bulk solid in the silo,
- a bulk solid recycling system that isolated vibration from the main silo,
- allow a continuous and smooth variation of the silo outlet width, whilst the bulk solid was arched or flowing,
- allow a continuous and smooth variation of the hopper half angle,
- toughened glass end walls to allow photography and visual inspection of the flow,
- a mechanically-isolated inter-changeable belt discharger and laser ranging unit.

2.1. The plane flow silo

The silo is shown in Figures 1 and 2. It had a fixed height of the silo 1.65m. The end walls were toughened glass, mounted 0.6m apart, and the distance between the vertical side-walls was 0.55m, giving an approximate volume of 0.6m^3. The main silo frame supported two independent sub-frames, which in turn supported the two walls of the converging section. With the total height of the silo fixed by the feeding system and laboratory ceiling, the height of the adjustable vertical section depended on the particular geometry of the hopper section. In terms of silo's width, the vertical section varied from 1 to 5 L/D ratios between the extreme slopes of the hopper section. To allow complete access to the under side of the silo and discharge box, the supporting frame had to be very stiff both, from the point of view of stress-free support of the heavy glass sides and the undistorted support of the sliding sub-frames while allowing the independent belt and drive system with scanning laser ranging device to move sideways so that each could sit directly under the slot without precipitating an arch collapse.

2.2. The variable geometry hopper wall sub-frames

Each sub-frame sat on three grease-lubricated ground stock slides and was moved by the rotation of a lead-screw. The hopper side was a sheet of stainless steel 304 with a 2B finish, that slid on a supporting frame, built to withstand the silo stresses. The sheet was secured to a lead-screw that allowed 50mm of in-plane movement of the wall. With this facility, the sense of the wall friction shear stress could be changed and its effect observed. With movement, both of the sub-frame and the in-plane hopper walls, the slot width could be adjusted in two ways, between limits of 20 and 200mm.

The two sub-frames also allowed the hopper half angle to be set between limits of 20–57.5°. The wall frame was pivoted at the base and the wall angle adjusted by raising a 50mm diameter tube on which, the upper end of the frames rested. At each end of the tube and passing through it, lead-screws driven by attached sprockets via a chain loop controlled the tube movement. Thus each screw was identically rotated.

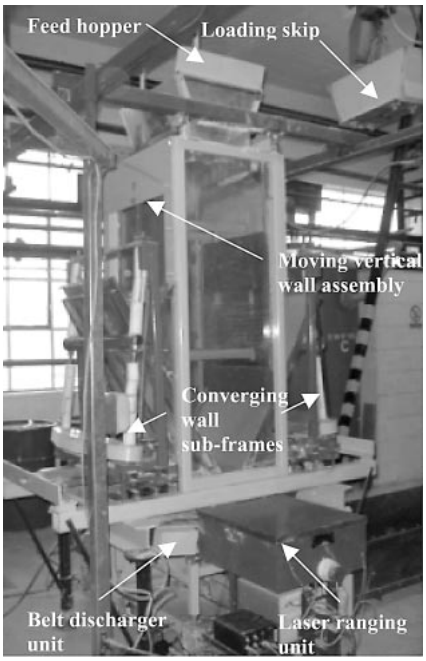

Figure 1. Photograph of the plane flow silo system

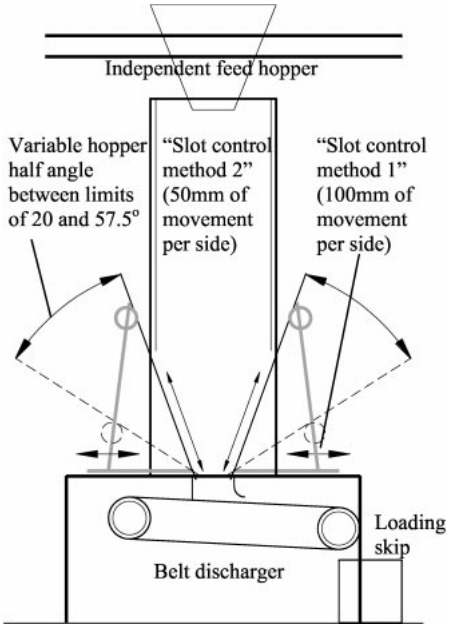

Figure 2. Schematic diagram of the plane flow silo system, illustrating the three converging wall sub-frame adjustment mechanisms

2.3. The belt discharger, the attached scanning laser-ranging device and discharge box

A controlled discharge of the bulk solid stored within the silo was achieved via a discharge drop box that fed the material onto a variable speed belt (see Figures 1 and 2). The belt conveyor drew across the slot and the angle of declination could be adjusted between 0–10° to ensure an even draw of bulk solid over the outlet area and promote the mass-flow pattern. The belt was supported on a stainless steel slider plate over the area under the outlet, rather than idlers, to minimise any disturbance that could be transmitted up through the bulk solid.

The belt discharger assembly and adjacent laser-ranging unit were mounted on a trolley and rails. When an arch had formed over the silo outlet the belt discharger could be pushed aside automatically bringing the laser into position for subsequent scanning. To facilitate this separation the discharge drop box was manufactured as two parts. The upper section of the discharge drop box was mounted to the silo frame, while the lower part was fixed to the belt conveyor assembly.

The measurement of the 3-dimensional surface of a cohesive arch was achieved by mounting a Micro-εpsilon displacement measuring laser sensor to an x-y table driven by stepping motors and controlled by computer (see Figure 3). For the measurements the system of co-ordinates used were defined as follows:

- the X co-ordinate represents the displacement along the length of the slot,
- the Y co-ordinate represents the displacement across the width of the slot,
- the Z co-ordinate represents the vertical displacement to the arch surface.

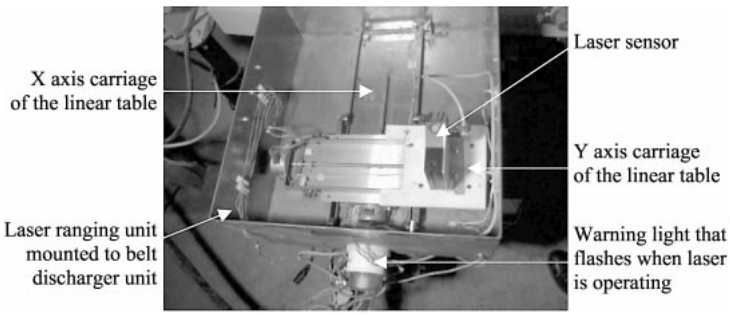

Figure 3. Photograph of the laser ranging unit

2.4. The feed hopper, bottom-emptying skips and hoist

An overhead plane-flow buffer feed hopper of 0.07m^3 capacity (shown in Figures 1 and 2) maintained a constant head of bulk solid in the vertical section of the test silo. To minimise vibrations transmitted to the silo structure during reloading, the feed hopper was mounted on an independent structure. Inside the feed hopper, a centrally mounted adjustable mass-flow insert acted as an impact breaker and allowed the outlet dimension to be minimised, so that the bulk solid just flowed through, with the consequence that the stress transmitted to the top bulk solid surface in the silo was minimised.

An overhead hoist and a pair of automatic bottom-discharge plane-flow skips of 0.05m^3 capacity were used to transfer the bulk solid discharged from the belt to the overhead feed hopper. The automatic discharge was achieved by lifting the skips via four chains which were connected to the corners of a pair of hinged trap doors forming the base. The trap doors were held shut by the tension in the chains during lifting. When the skip was lowered onto the feeder hopper, the tension in the chains relaxed and the self-weight of bulk solid opened the doors, allowing discharge.

3. Summary of all tests and observations

The failure properties of the powders used were published in [8]. The basic method of filling the silo was strongly controlled by the system. Influencing the severity of the deposition, *i.e.* gentle or dumped, was attempted, but the scale of the system left little room for control without major modification. As the feed hopper was there to control the level of the bulk solid of a full silo, it had no gate. It follows that in the early stages of filling the bulk solid fell straight to the bottom of the silo. In consequence, the deposition was mostly affected by the nature of the bulk solid. The olivine sand being coarse and heavy (approximately 1450kg/m^3) probably compacted heavily. The fly ash had a moderate bulk density (approximately 600kg/m^3) but contained and entrained more air. On striking the bottom of the silo, there was a certain amount of fluidisation and so, most likely, produced a heterogeneous density and stress field. The hydrated lime fluidised so readily and created such hazardous clouds of dust that it had to be filled manually by small buckets, by-passing the normal feeding system. While this bulk solid was similar to fly ash (approximately 600kg/m^3) it probably compacted the least on filling, as the de-aeration time was longer.

The following points summarise a number of observations which, to the best of the authors' knowledge, have not been reported previously and whose detailed reporting is not possible here due to space limitations. Only the filling results are covered in detail and immediately follow the points outlined below.

1. With the all three bulk solids and the silo in a mass-flow and non-mass-flow configuration, the undisturbed top surface descended as usual for mass flow. On reaching a level, approximately one silo width above the geometric transition, a fairly uniform V-channel developed in the top surface. Its orientation was a surprise as was orthogonal with the length of the outlet. As the channel arrived in the region of the transition, the usual mass-flow V-channel appeared forming a cross with the original channel. No explanation can be offered for this phenomenon. This behaviour prompted the removal of the discharge box and the belt to enable a full bore emptying of the silo, in case either was the cause of this effect: neither was responsible.
2. On the commencement of emptying a full silo and approximately for the upper half of the silo, all bulk solids moved out of contact with the glass wall. An optical illusion was discounted when particles were observed to fall down the narrow space. Even during continuous filling of the silo the bulk solid from the feed hopper top surface spilled and spread, so that the top surface was in contact with the glass, but separation still occurred some 150mm below the top level. Contact was re-established about the level of the transition. This has considerable implications for the wall stresses of plane flow silos, but this behaviour *may* only occur with full-length slot outlets with vertical end walls.
3. The visual observations of behaviour at the glass walls did not prove to be as valuable as anticipated, as fillets of stationary material built-up in the silo corners. Hence observations at the wall were restricted and the central behaviour could not be verified.
4. In a fully mass-flow geometry, the inclined and curved slip lines created during flow and seen at the wall, were so tight that they were difficult to see. In contrast, the slip lines, which formed when the geometry was close to the transition region between mass flow and non-mass flow, were vertical and widened to such an extent that in some places gaps were upto 0.5cm wide. In the obviously non-mass flow region, the slip lines become tight again, clearly diverging in the region of the outlet and appearing to become asymptotically vertical at about the transition.
5. As observations of the flow patterns were not conclusive, the cautious term, non-mass-flow has been used. Certainly, core flow does not occur in full plane-flow non-mass-flow silos and this is consistent with their theory, as there cannot be any curved channel to enable vertical internal wall stability. However, there are observations that support an internal mass-flow mechanism in non-mass-flow silos. Internal mass flow is a flow pattern which, under certain conditions, mimics mass flow in core/funnel flow and flat-bottomed silos, if the outlet is large enough. This flow pattern may not have the stability of mass flow at a hopper wall, but the type of stress field and stress distribution are the same.

6. The critical outlet widths for the "at filling" and "at emptying" conditions have been compared with critical outlet widths that were determined following the Jenike design method in [8]. In summary, the "at emptying" slot widths were industrially insignificant in size (less than 50 mm), while the magnitude of the slot widths predicted by the Jenike design method were more consistent with the "at filling" critical slot widths.

4. Detailed results of the "at filling" arching experiments

This section describes a representative selection of the "at filling" arching experiments and their results in detail. Having filled the hopper and allowed time for de-aeration, as appropriate for the bulk solid, the belt discharger started and the gate at the bottom of the hopper was withdrawn. At the start of the tests with olivine sand and glycerine the minimum slot width was approximately 50 mm. As it became clear that arching widths were much greater, initial widths for the other two materials were larger, as can be seen from the figures showing the arching profiles.

The readings obtained with the laser-ranging unit are presented as profiles and contours (as defined in Figure 4), the former being a cross-section of the arch, while the latter is a section through the length of the arch. While a contour may be taken at any set distance from the centre-line of the slot outlet, the contours presented below are only at the centre-line, as contours at other positions are too erratic to be of analytical value. The results in this chapter follow the progress of the arch profiles and the central contour as the slot width is enlarged from its initial value to the last arch before total collapse and subsequent flow.

There is insufficient space to show all the arches for all 5° increments of hopper half angles, so only the 20° mass flow and the first non-mass-flow half-angle results are presented. A summary of the "at filling" tests presented is given in Table 1 below, while Table 2 gives some of the salient failure properties of the materials used.

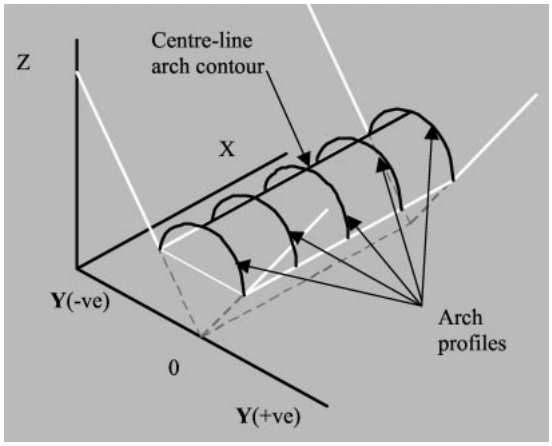

Figure 4. Co-ordinate system for the arch surface measurements

Table 1. Conditions under which experimental arches were formed

Bulk solid	Hopper half angle	Initial slot width	Critical slot width	Flow pattern
Olivine sand	20°	51mm	82mm	Mass-flow
Fly ash	20°	58mm	106mm	Mass-flow
Fly ash	20°	106mm	120mm	Mass-flow
Fly ash	20°	150mm	<150mm	Mass-flow
Fly ash	45°	38mm	112mm	Non mass-flow
Fly ash	45°	110mm	136mm	Non mass-flow
Fly ash	45°	150mm	>150mm	Mass flow
Hydrated lime	20°	85mm	158mm	Mass-flow
Hydrated lime	40°	42mm	108mm	Non mass-flow

Table 2. Bulk solid failure properties

Bulk solid	Angle of wall friction (stainless steel)	Angle of wall friction (glass)	Effective angle of friction	Gradient of linear failure locus
Olivine sand	24	11	38	29
Fly ash	18	11	40	30
Hydrated lime	26.5	27	42	22

4.1. Results from the 20° *mass-flow hopper*

With the silo at the 20° mass-flow hopper setting, all the first arches had a similar shape, were generally fairly smooth and clearly failed in tensile fracture. In these series of measurements the slot was enlarged by slowly moving each sub-frame in turn, approximately 2.5mm at a time. This was continued until the next partial collapse of the arch occurred. After the belt had cleared the fallen material, it was pushed aside, bringing the laser-ranging device under the slot. The device could only measure one third of the slot in one scan, two thirds of the slot was measured in two scans. The final third was not measured, as no mechanistic difference in the arch profile could be seen through either glass wall. A partial collapse only occurred occasionally, so as the slot was widened, bulk solid, en-masse, slid down the walls and initially protruded through the slot. Subsequent collapse behaviour varied slightly with each material. With the olivine sand, it always protruded before partially collapsing and, as the slot became wider, the arch became asymmetrical, as seen in Figure 5a. As with all the figures, all the arches are displayed relative to the same hopper vertex point. In the last partial collapse, it is seen that the asymmetry switches along the arch. It is seen that there are four stages to the critical arch, whose dimension is shown by the upper pair of horizontal lines (obviously, with no arch attached). The contours of the different arches are seen in Figure 5b. Note that there is only a small variation in height along the slot.

In the original figures of this project the different arches were distinguished by colour coding, but in black and white the different profiles become a profusion of lines. The system of coding used in the following figures is the best system found, though only just adequate. The profiles and their stage numbers are presented alternately

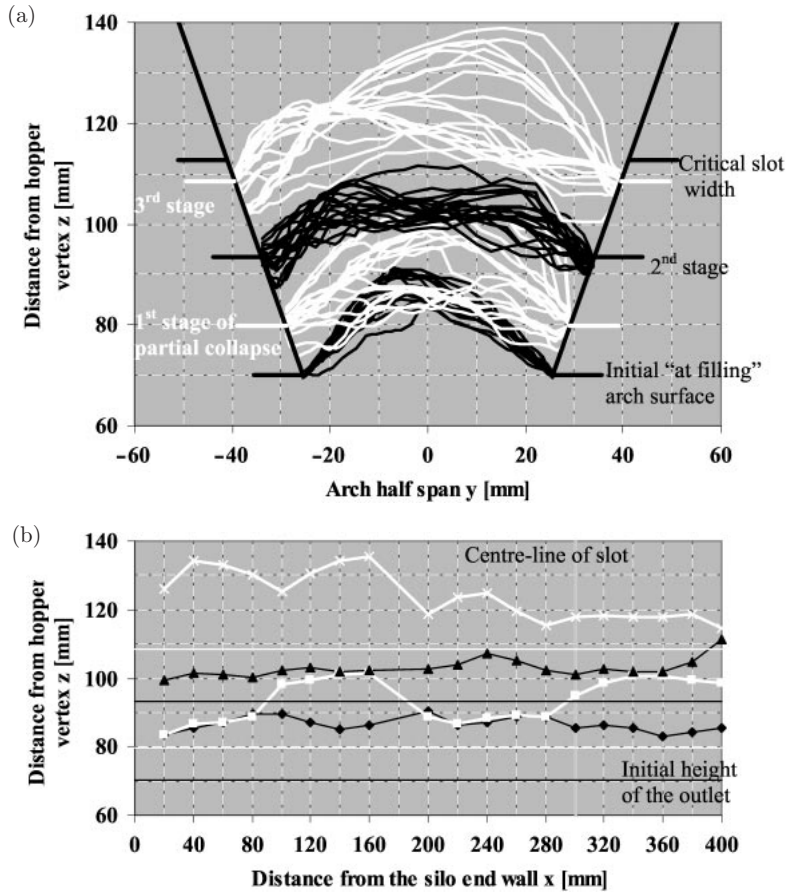

Figure 5. Partial arch collapse stages for cohesive olivine sand in a 20° half-angle mass-flow plane-flow silo: (a) arch profiles, (b) arch contours

in black and white, with the white numbers on the left corresponding to the white profiles.

While the fly ash in Figures 6a and 6b presented basically the same behaviour, the one significant difference from the olivine sand was that protrusion had gone into reverse, *i.e.* the arch abutments had moved up from the hopper slot edge, a behaviour that we have called *wall-walking*. As the laser can only see vertically, only a portion of the arch is visible, but, of course, the arches were visible through the glass. Had this behaviour been reported previously, we would have arranged the scanning device to be θ, x. The arches profiles and contours show the maximum slot width for total collapse (critical arch) occurring in eight discrete stages. For this hopper geometry and therefore the filling stress distribution, the maximum arch may be regarded as a critical arch but, as we shall see later, a wider initial slot width will change its stress distribution and a different critical arch will result.

The third bulk solid, hydrated lime, filled more gently by upturning a bucket just above the current surface to minimise the obnoxious dust, showed a similar behaviour to the fly ash. The differences, see Figure 7a, were more protrusion and less wall-walking relative to the fly ash behaviour.

(a)

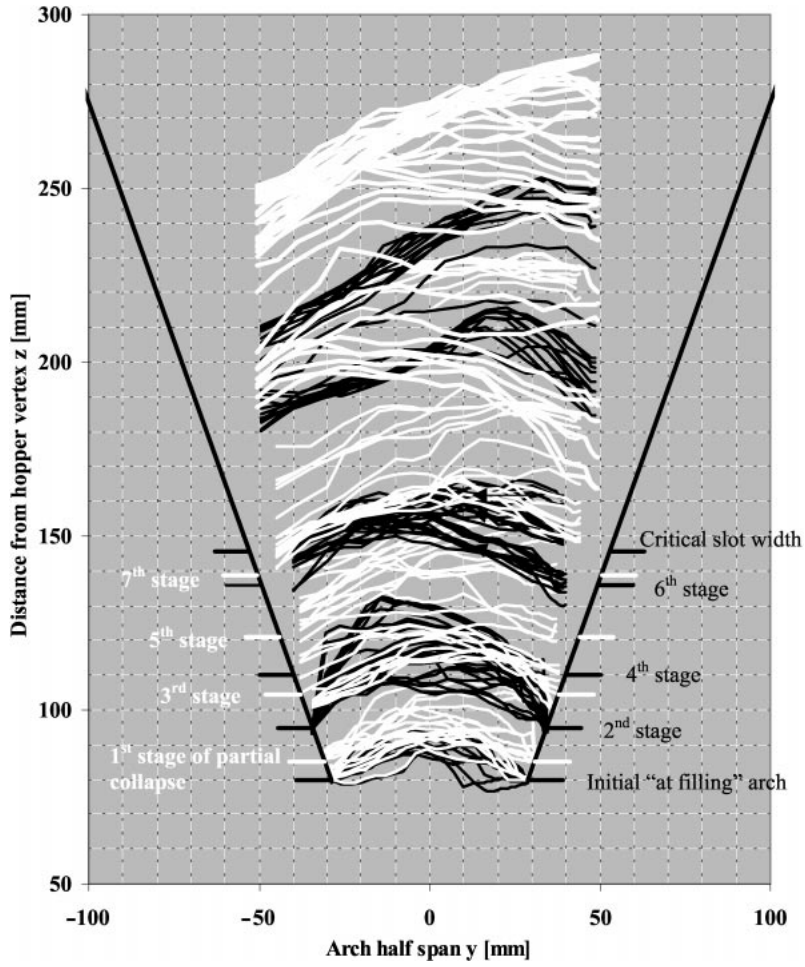

Figure 6. (a) The arch profiles of the partial collapse stages for fly ash in a 20° half-angle mass-flow plane-flow silo

For the fly ash and the hydrated lime, (see Figures 6a and 7a) where the arch abutment was obscured due to wall-walking, it follows that the slot width is not the same as the effective span. The *effective span* is defined as the average value of twice the distance of the lowest arch abutment of a profile from the slot centreline. This definition is necessary as most profiles are asymmetrical and their abutments are not always at the same level. The effective span was measured approximately by viewing the lowest arch abutment through the glass end walls while, at the same level, measuring the distance between the hopper walls against the glass. Several measurements were made at points along the length of the slot to provide the average values. These values were used to construct Figure 8.

The above tests have determined the critical slot width and the critical effective arch span for three different materials, but only after the contents had slid down the hopper wall for a significant distance. If now the experiments were repeated, except that the initial outlet had been set at the critical effective span as previously measured, would this dimension remain the same and the arch collapse immediately?

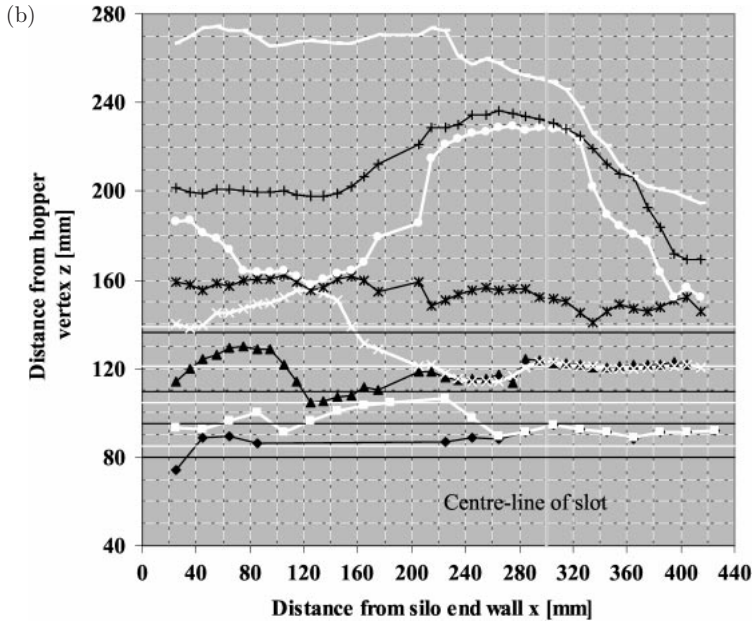

Figure 6 – continued. (b) The arch contours of the partial collapse stages for fly ash in a 20° half-angle mass-flow plane-flow silo (Note: double vertical scale)

This would not be expected, as two system variables would be different. Firstly, during filling in the region of the gate, a greater vertical normal stress would be possible as the proportion of force lost to the wall is smaller. This larger stress will cause higher density and strength and a larger arch span could be expected. Secondly, the work done on the bulk solid by the shear stress at the wall and the distance travelled may have strengthened the bulk solid. The significance of this effect was studied, next.

For this new set of tests fly ash was chosen. The initial slot width was adjusted to the value of the last critical slot width and the same experimental procedure repeated. The results are shown in Figure 9. The figures show that the span can indeed support an arch and, in addition, support two further partial arch collapse stages. The new critical width was 120mm, an increase of 13% over the previous test series. This effective arch value is at least 8 times the critical arch "at emptying". As the critical effective span was still larger than the initial slot width, the test was repeated again with an initial slot width of 150mm but, on removing the gate, flow commenced immediately.

Figure 10 shows the comparison of all initial arches for the first test series of the three materials and the initial arches for the second test series of wide outlet for fly ash and lime. Both axes are normalised so that the arches are shown with the same dimensionless span, with only the arch shapes being different. There are too few data from which to draw conclusions, but it is interesting is that the wide arch has an almost identical dimensional similitude with the narrow fly ash arch. The other two arches are also very close and all are reasonably symmetrical: a factor not seen in subsequent arches.

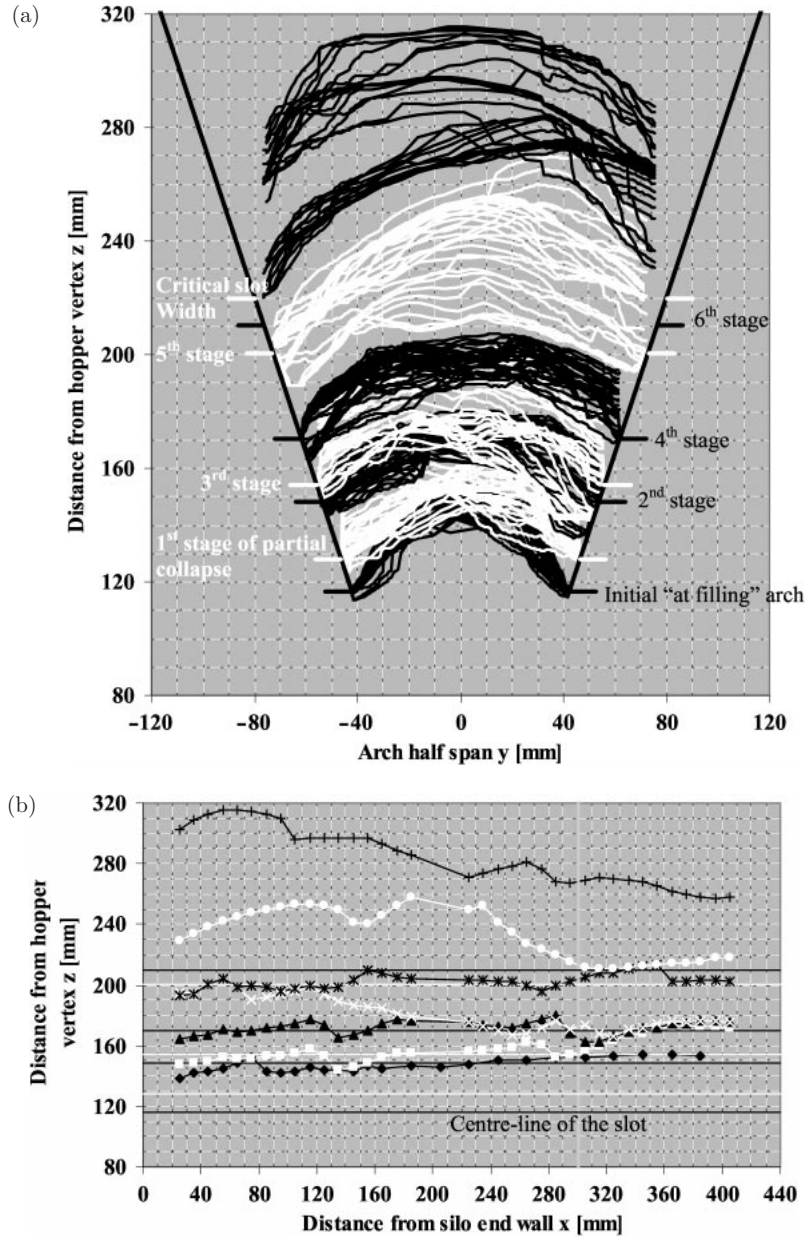

Figure 7. (a) The arch profiles of the partial collapse stages for hydrated lime in a 20° half-angle mass-flow plane-flow silo; (b) the arch contours of the partial collapse stages for hydrated lime in a 20° half-angle mass-flow plane-flow silo

4.2. Results from the non-mass-flow hopper

With the volume of experimentation it was not possible to investigate the transition from mass flow to non-mass flow. At the completion of "at filling" and "at emptying" test series, the half angle of the hopper was increased a further 5° and another series commenced. It was, therefore, not possible to report how sharp the transition was, other than it took place within 5°. For the fly ash, the transition

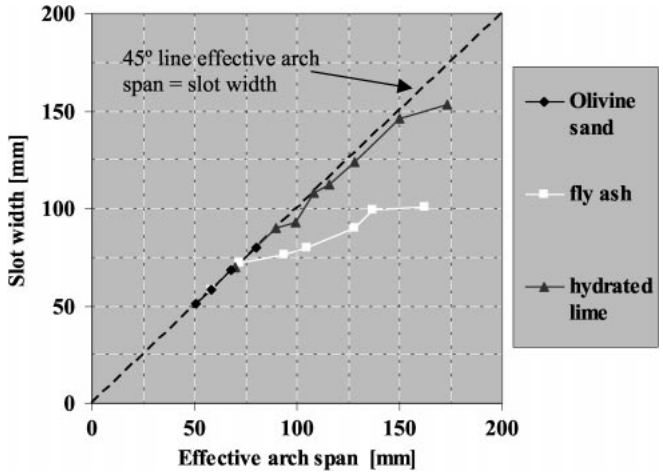

Figure 8. Relationship between the "at filling" slot width and effective arch span for olivine sand, fly ash and hydrated lime, as the slot width is increased from the initial value to the critical arch

occurred between 40° and 45°, while for the lime, it occurred between 35° and 40°. The term non-mass flow has been used to err on the side of caution. As the objectives of the project concerned only arch profiles, no devices were installed to monitor flow patterns and velocity distributions. However, general observation was possible through the glass walls. During emptying, the level top surface of the material remained level as in mass flow, except for stable fillets of material in the corner of the vertical section. These remained, even when all the other material had emptied. There was also another exception. Within half a metre of the maximum fill height, the top surface developed a fold about 150mm across and about 80mm deep. As mentioned in a previous section, its orientation was orthogonal to the slot. As the surface descended further, the conventional fold developed aligned with the slot. Eventually this grew to obliterate the initial fold. Its curved nature of the sides of the growing fold is characteristic of mass flow. Core flow (defined as a stable near-vertical flowing core) always presents a straight sloping flow surface to the centre of the cone. These features are positive identifiers of mass flow, internal mass flow and core flow patterns. Funnel flow, like non-mass flow, cannot have an identifier as it is an indefinite mixture or transient flow patterns. Although the non-mass-flow plane-flow silo appears to attempt core flow, the slip planes of the incipient core are essentially planar and cannot be sustained through a lack of horizontal curvature to ensure stability.

Returning to the previous thread of observations, further descent of the top surface while still above the silo transition revealed a straight inclined surface of stationary material against the vertical wall between the corner fillets of material. This is a characteristic of internal mass flow where the mechanism of flow and the stress distribution is identical to flow against a hopper wall, *i.e.* mass flow. With the olivine sand and the fly ash, the fillets were approximately 300mm radius. As this is a significant proportion of the total width, the authors' are exercising some caution by using the term non-mass flow. If internal mass flow had been established, it was impossible to determine if this commenced immediately "at emptying" with the silo full or, finally appeared after passing through a funnel flow transition.

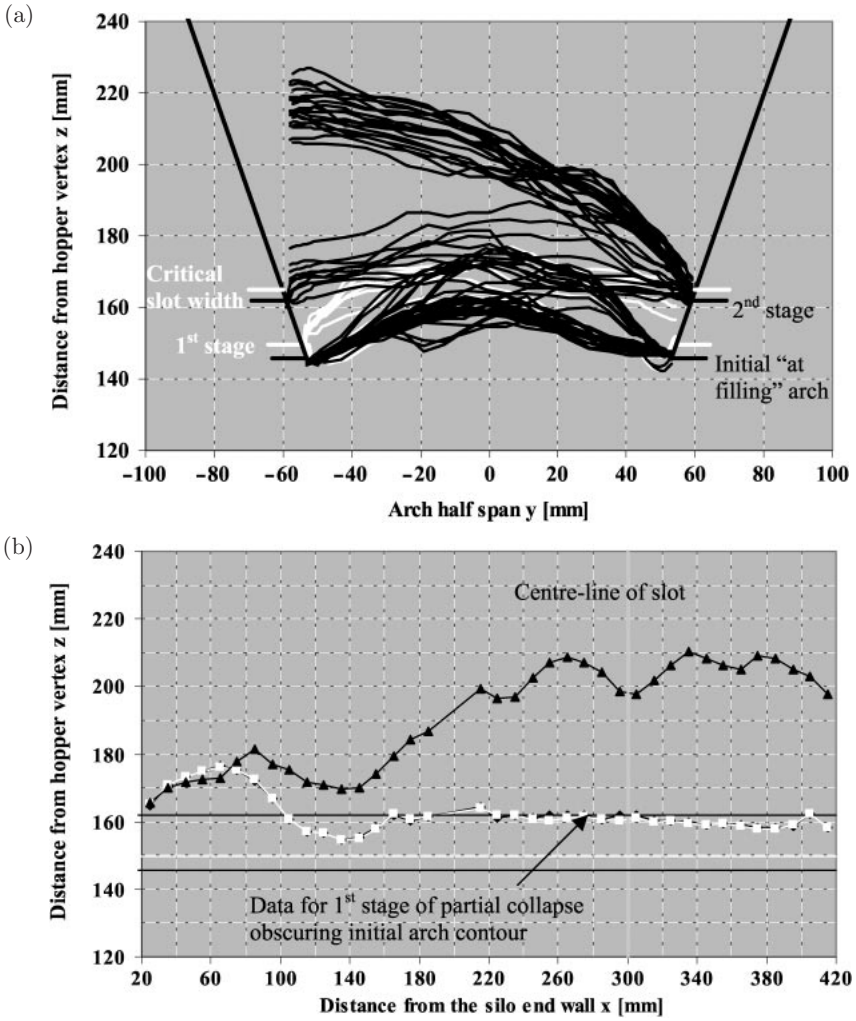

Figure 9. Partial arch collapse stages for fly ash in a 20° half-angle mass-flow plane-flow silo, with the first of the enlarged initial slot widths: (a) arch profiles, (b) arch contours

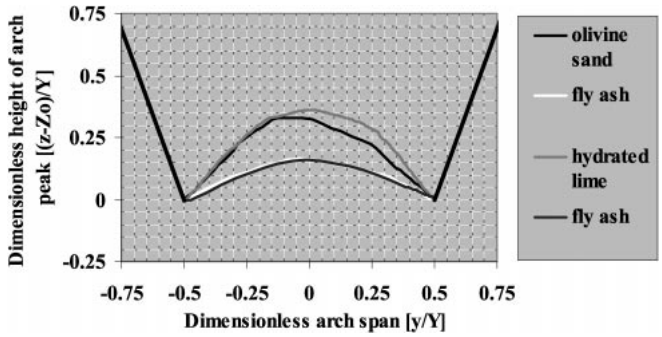

Figure 10. Dimensionless mean profiles of the initial "at filling" arches for olivine sand, fly ash and hydrated lime

Figure 11 displays the results for fly ash with the hopper at a half angle of 45°. While the arch profiles quickly established an asymmetric shape, as did the mass-flow arches, the dominant slopes of the non-mass-flow arch were steeper. After the second stage of partial collapse, a pair of roughly vertical slip planes visible through the glass end walls. They extended from the converging walls and intercepted one another out of the field of the figure with an elliptic type curvature. In between these slip planes, slumped material formed the arch. As the slot was widened further, the vertical planes moved apart and between the third and fourth partial collapse, a large slab of material fell leaving a larger arch enclosed by the vertical slip-planes. In the final arch, the measurements were incomplete, as the arch had exceeded the range of the laser, resulting in the horizontal line at the top of the figure.

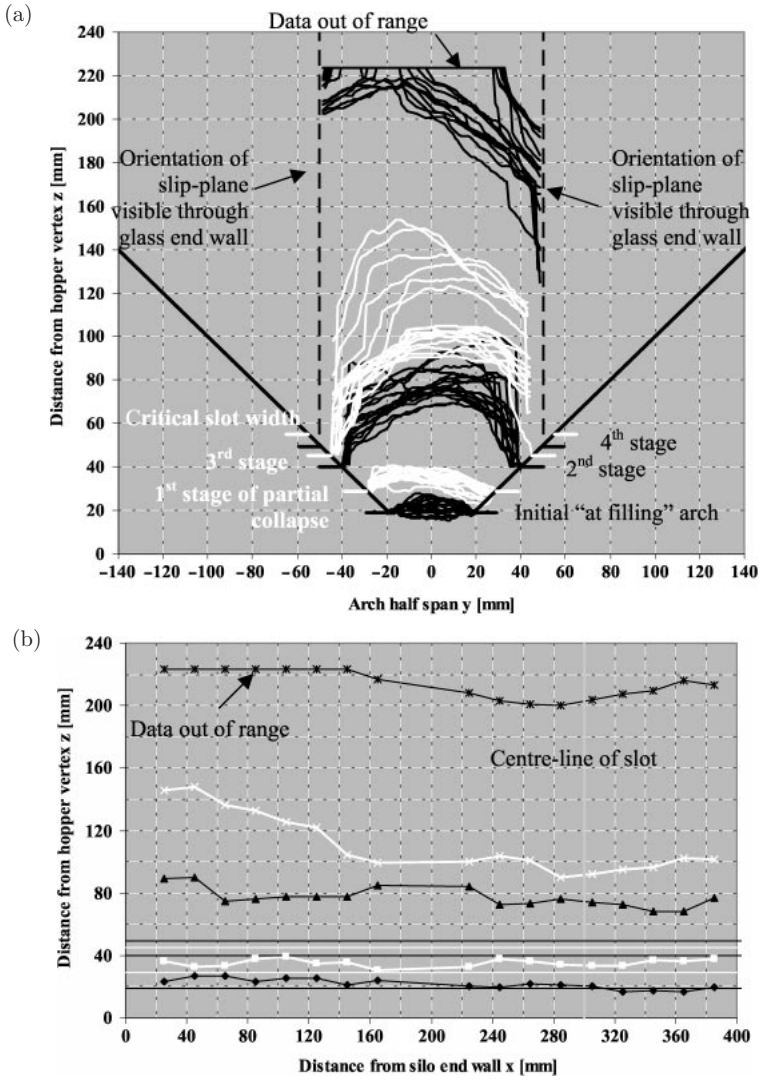

Figure 11. Partial arch collapse stages for fly ash in a 45° half-angle non-mass-flow plane-flow silo: (a) arch profiles, (b) arch contours

Although the initial slot width began at a smaller value, there were less partial collapse stages. Despite this, the critical slot width was close to the mass-flow value. However, in this case, the critical effective span was only a little larger than the critical slot width. The contours in Figure 11b were generally more horizontal in nature than their mass-flow counterparts.

For the lime, the transition to non-mass flow occurred earlier: Figure 12 shows the test results for a half angle of 40°. The profiles and contours in these figures have a slightly different character from the fly ash, but the character of the near vertical slip-planes was the same with extending from the converging wall and observed after the second stage of partial collapse. The last but one partial collapse, (a white line in Figure 12a) shows a steep slope to the arch on the left side with many of the profiles to the right coinciding with the previous partial collapse. Clearly, the final partial collapse occurred mainly on the left side of the profiles. When the Figure 12b contours are examined, the last two contours show very slight differences at the centre line. It follows that, while the centreline remained almost intact, there was a major fall of the material to its left and also a small breakaway to its right. These last contours were also different from those of the fly ash, in that there was a significant height variation. As with the fly ash, the arch profiles terminate at near-vertical walls that had an elliptical type curvature. Perhaps the most surprising feature of the final arch profiles in Figure 12 is that 50% of the profiles are roughly horizontal for a span greater than the slot width: an exaggeration of the fly ash final arch and very different from mass-flow arches.

As in Section 4.1, the fly ash tests were duplicated with a larger initial slot width, 110mm. In this case, there were only two partial collapses before critical slot width, which occurred at 136mm, see Figure 13. This test was again repeated for an initial slot width of 150mm, but flow commenced immediately.

5. Discussion of results and mechanisms

The main surprise to the authors' in this work was the considerable irregularity in every aspect of arch characteristics: its asymmetric profiles; its irregular contours and the irregularity of the sequence of partial collapses and in the case of mass-flow hoppers, its wall-walking. All these aspects point to a very heterogeneous state or, the presence of two or more failure mechanisms which lead to very close failure conditions, such that only small variations in the bulk solid condition at similar levels in the hopper can lead to different types of local failure.

The most consistent feature of the work was the initial arches, but even they only partially met the common concept of the shape of an arch.

One persistent feature of all the "at filling" arches is that all the partial collapses are fractures. The main body of the bulk solid in the hopper remains solid and integral. It can slide down the hopper, while the walls are in the process of being expanded, without loss of integrity, apart from occasional very intermittent rain of very small lumps of material as the critical arch dimension is approached. From these observations, it is clear that the main body is elastic and significant portions fracture from it.

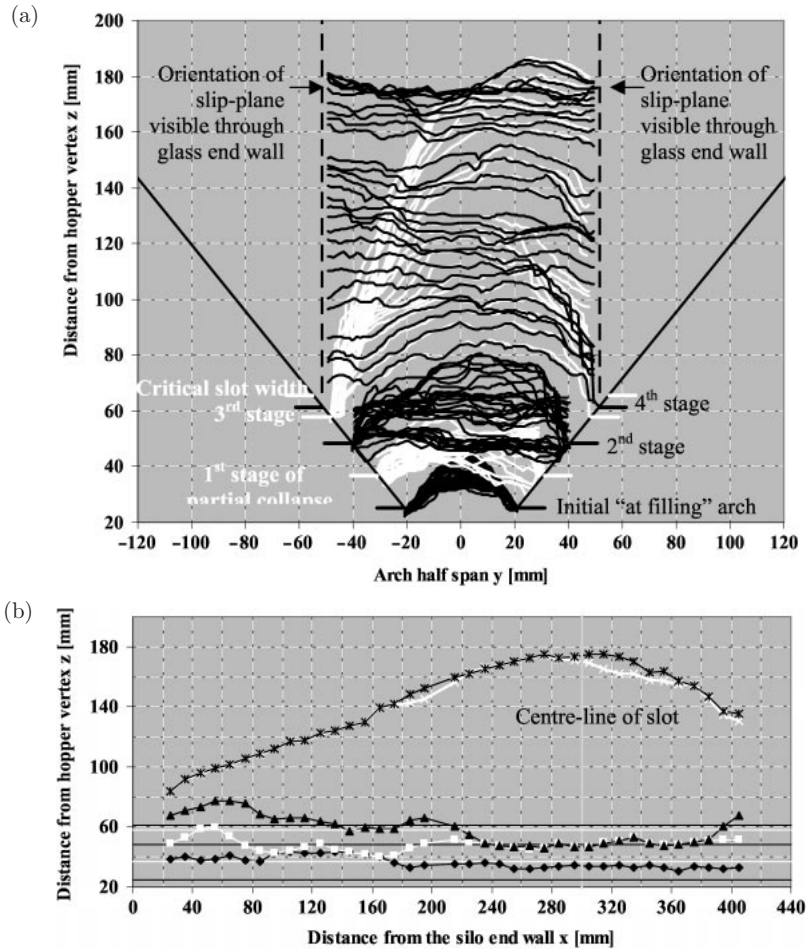

Figure 12. Partial arch collapse stages for hydrated lime in a 40° half-angle non-mass-flow plane-flow silo: (a) arch profiles, (b) arch contours

The generally accepted notion in mass flow is that slip takes place at the abutment of a collapsing arch destroying its stability, but in these experiments, the movement outwards of the walls meant that significant sliding had already taken place before an arch collapsed. Clearly, "at filling" another mechanism or mechanisms are at work.

The most important finding of this work is that the filling condition of a silo is the worst case from the point of view of reliable flow under gravity and without a flow-promoting device. Almost certainly, the reason that this has not been found as the result of using the Jenike method of design over a few decades is the considerable over-design that occurs partly in the design, but mainly in the measurement and the analysis of results. Unfortunately, our knowledge of the state of stress and its distribution in the region of the outlet for the "at filling" case is totally inadequate to formulate an alternative design method. The major difficulty, as we will see in a moment, is the problem of predicting the effect of the deposition of the bulk solid during filling, which involves such considerations as; the interactions between air,

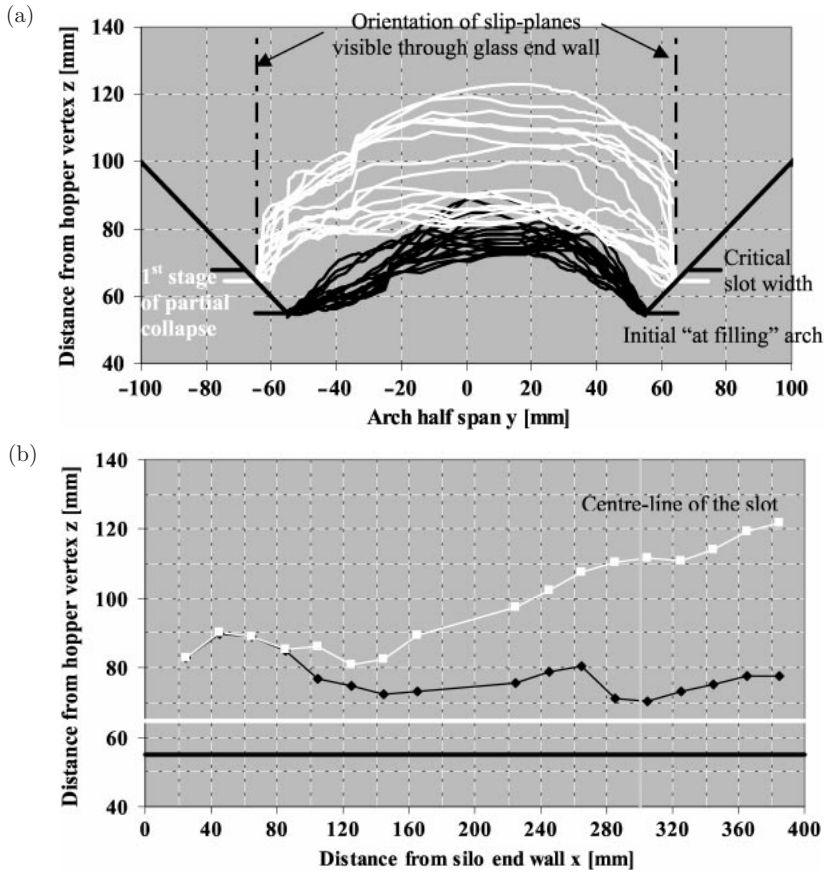

Figure 13. Partial arch collapse stages for fly ash in a 45° half-angle non-mass-flow plane-flow silo, with the first of the enlarged initial slot widths: (a) arch profiles, (b) arch contours

solid, its tribo-electrification and the geometry of the hopper containment, as the bulk solid is dropped, poured or blown in.

In a recent study [9] of the one dimensional density distribution in an axisymmetric mass-flow model silo, 280 mm in diameter and made from 25 mm separable slices located with each other by dowel pins, two methods of filling were used. In the first method, powder was sieved above the silo, allowing the powder to rain gently down into it. Consequently, compaction of the powder was uniaxial and by self-weight, to the extent of the modification by the friction of the silo wall and the hopper geometry. This represents one extreme condition of filling. In the second method, the bulk solid was filled into a similar diameter-sized container and its contents were then dumped into the silo. The silo became full with four dumps. In each case, the top of the silo was strickled level with a straight edge. A two-part tray was then attached round the silo and a 25 mm slice removed and the powder collected. This was continued for all layers of the silo until it was totally dismantled. From the weight of powder from each layer and the accurate individually-determined volume of each layer, the density in each silo slice was calculated and plotted as seen in Figure 14. The Janssen curve for the silo vertical section is clearly seen, showing a density dif-

ference due to the filling methods, roughly averaged, of no more than 5%. In the hopper section the different distributions could not be more marked. For the dumped distribution, from the immediate vicinity of the outlet and for some height into the hopper, the density increases and this must create a stronger bulk solid, allowing an arch to withstand the increasingly destructive stress due to a greater span. Exceeding the peak density, the bulk solid would lose strength and the arch would quickly collapse.

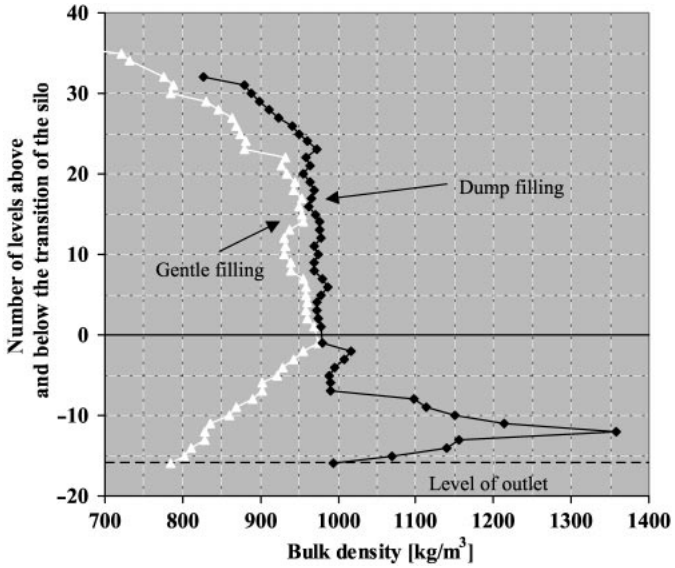

Figure 14. The density distributions in a model silo following two different methods of filling

If the density distribution of the bulk solid in the dump-filled pilot-plant silo is of a similar nature to that in Figure 14, this readily explains the wall-walking of the fly ash and hydrated lime arches. However, it is difficult to explain why the olivine sand did not wall-walk, perhaps the liquid wetted particle contact points made the bulk solid less brittle. When the density effect on an arch span is allowed for using the conventional arch span equation and normalised roughly with the density ratio, relative to the other two materials, the critical span increases by approximately 250%, bring the equivalent span to 200 mm, exceeding the critical spans of the other materials.

Another aspect of this work impacting on silo theory, is that it demonstrates that the onion ring approach to arches, almost universally used as the basis of modelling arches, clearly does not apply, except for initial stable arches. All pre-critical arches for mass flow are dominantly asymmetric, so this would suggest quite a complex failure mechanism. The failure of arches in the non-mass-flow hopper clearly occurs by a different mechanism and yet, the critical arch span is virtually identical to its mass-flow counterpart.

Direct comparisons between the mass-flow arch spans and the non-mass-flow arch spans should be made with considerable caution, as the hopper angle is likely to have a significant effect of the fill density value and its distribution.

6. Conclusions

As all the previous literature has given an arch shape similar to the form in Figure 4, the results reported here totally destroy the conventional notion of arch shape used in all critical arch theories. They have also destroyed the notions that: (a) emptying a small amount of bulk solid from a silo converts the stress field to an emptying state (though still a sensible procedure while filling), and (b) that the worst case for silo design is an instantaneous emptying state. The work has shown the necessity to clearly identify the state of the bulk solid before making assumptions concerning stress fields, arching theories of collapse and observations on silo flow patterns. These are "at filling", "at transition" and "at emptying".

If there is one main observation and one main conclusion from this paper, it must be the enormous variability of the arch shape in plane flow and that bulk solid behaviour in silos is not more than half understood.

References

[1] Jenike A W 1964 *Utah Univ. Eng. Exp. Stn. Bulletin* **123** 84
[2] Wright H 1970 *Bunker Design for Iron Ores*, Dissertation, University of Bradford, UK
[3] Blanchard M H and Walker D M 1967 *Coal flow – arching in experimental hoppers*, C.E.G.B., Sci. Services
[4] Eckhoff R K and Leversen P G 1974 *Powder Technology* **10** 51
[5] Clauge K 1973 *The Effects of Stresses in Bunkers*, Dissertation, University of Nottingham, UK
[6] Enstad G G 1985 *Int. J. Bulk Solids Storage In Silos* **1** (4) 126
[7] Katalymov A V and Polunov U L 1990 *Powder Handling and Processing* **2** (4) 307
[8] Berry R J, Birks A H and Bradley M S A 2000 *Proc. 3rd Israeli Conf. for Handling and Conveying of Particulate Solids*, The Dead Sea, Israel, pp. 117–128
[9] Moore S 2003 *An Investigation into the Effects of the Method of Deposition of Cohesive Powders on the Stress Distribution within a Model Silo Using Mechanisms of Compaction*, MSc Thesis, University of Greenwich